Electron Trajectory Calculations Using the Vector Potential

Raymond Browning
15 Dec 2016

In designing the microscope we have been hampered by the lack of a consistent theoretical description of the electron trajectories as they leave the magnetic field. There are two completely different descriptions, first, when the electron is travelling in the magnetic field (the adiabatic region), and second as it leaves the field (sudden approximation). Within the magnetic field we use the conventional view of the electron trajectory along field lines under the Lorentz force. In the Lorentz region the canonical momentum of the electron from the vector potential is not conserved. When the electron leaves the magnetic field as the field is suddenly terminated by a ferromagnetic shield, the deflection is calculated from the conservation of the canonical momentum from the vector potential at the point of termination. These two descriptions are valuable, but are disconnected in the very region we ae interested in for developing the electron optics. This disconnect prevents us having any unified design metrics for creating a new microscope, or understanding the possible modes of operation of the current design.

There is no mathematical description of electron trajectories travelling in a vector potential field in the literature. Typically, the electron is assumed to move adiabatically within a magnetic field and the Lorentz force equation used to predict its behavior. There is large literature concerned with electron and ions moving in a magnetic field, involving sophisticated, and approximate, mathematical descriptions, as the electron trajectories move off the field lines. These mathematical descriptions are typically used in the realm of plasma physics. We have not found the literature to be of use for microscope design. In fact, the properties of electron trajectories moving through an aperture in a ferromagnetic shield have not been explored. The VPPEM is a unique electron optical system.

To help our understanding of VPPEM technology we have created a new description of the electron trajectories using first principle calculations of the vector potential. This appears to be valuable, and we are hoping to develop a metric to aid in the design of new microscopes.

In the VPPEM the momentum from the vector potential is converted into the off-axis momentum of an angular image by suddenly terminating the field. To understand this action in detail we have created a computer program to simulate an electron trajectory where the Lorenz force has been rewritten using the forces due to changes in the vector potential.

The vector potential is given by equation 1:

$$\mathbf{A}(\mathbf{r}) = \frac{\boldsymbol{\mu_0}}{\boldsymbol{4\pi}} \int_{\boldsymbol{\Omega}} \frac{\boldsymbol{J}(\acute{\mathbf{r}})}{|\mathbf{r}-\acute{\mathbf{r}}|} \mathrm{d}^3\acute{\mathbf{r}} \qquad (1)$$

Where $\mathbf{A}(\mathbf{r})$ is the vector potential at position $\mathbf{r}$, $\boldsymbol{J}(\acute{\mathbf{r}})$ is the current density at position $\acute{\mathbf{r}}$, and $\boldsymbol{\Omega}$ is the volume of the current density.

Integrating Equation 1 around a circular loop of current gives a vector potential field that is zero on the axis, and is a maximum at the radius. The direction of the momentum is around the axis in the direction of the current. The curl $(\boldsymbol{\nabla}\times)$ of this field distribution is a constant. From Maxwell's equations the magnetic field is:

$$\mathbf{B} = \text{curl } \mathbf{A} \qquad (2)$$

The magnetic field within a (long) solenoid is a constant.

The canonical momentum of a charged particle in a magnetic field is:

$$\boldsymbol{p} = m\dot{\mathbf{r}} + q\mathbf{A}(\mathbf{r}) \qquad (3)$$

Where **p** is the momentum, m is the electron mass, and q is the electron charge.

Using standard analytical mechanics we write the Lagrangian for an electron in a vector potential field:

$$\mathbf{L} = \frac{m}{2}\dot{\boldsymbol{r}} \cdot \boldsymbol{r} + \dot{q}\boldsymbol{A} \cdot \dot{\boldsymbol{r}} \qquad (4)$$

After using Lagranges's equations:

$$\frac{d}{dt}\frac{\partial L}{\partial \dot{x}} = \frac{\partial L}{\partial x} \qquad (5)$$

We obtain the resolved force equations:

$$F_x = q\left[\dot{y}\left(\frac{\partial A_y}{\partial x} - \frac{\partial A_x}{\partial y}\right) + \dot{z}\left(\frac{\partial A_z}{\partial x} - \frac{\partial A_x}{\partial z}\right)\right] \qquad (6)$$

$$F_y = q\left[\dot{x}\left(\frac{\partial A_x}{\partial y} - \frac{\partial A_y}{\partial x}\right) + \dot{z}\left(\frac{\partial A_z}{\partial y} - \frac{\partial A_y}{\partial z}\right)\right] \qquad (7)$$

$$F_z = q\left[\dot{x}\left(\frac{\partial A_x}{\partial z} - \frac{\partial A_z}{\partial x}\right) + \dot{y}\left(\frac{\partial A_y}{\partial z} - \frac{\partial A_z}{\partial y}\right)\right]$$

(8)

The force equations are used to track trajectories in a simple model system. Figure 1 shows a model system with two current loops.

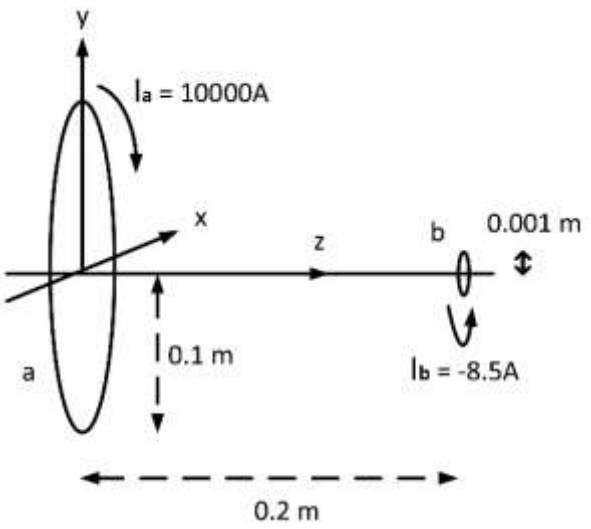

Figure 1. Two current loop model for electron trajectory simulations using the vector potential. The current in loop **b** is opposite to the current in loop **a**, and reduces the total field at the center of loop **b** to zero.

We have arranged the respective currents in the current loops to produce a zero field at the center of the second loop. After passing the second loop the field is numerically set to zero to simulate the electron passing through a ferromagnetic shield.

All terms in A_z are zero in equations 6-8 because there is no resultant vector potential out of the plane of the current loops. For any position in the electron trajectory Ax and Ay, and their differentials are numerically calculated by integrating equation 1around the current loops.

The initial field at the center of loop **a** along the z axis, B_z, is calculated from the curl of the vector potential, or simply:

$$B_z = \frac{\partial A_x}{\partial x} + \frac{\partial A_y}{\partial x} \qquad (9)$$

From the dimensions and current shown in Figure 2 the initial B_z = 0.06283 Tesla, in agreement with the standard calculation. The shape of the axial B field with z is shown in Figure 2.

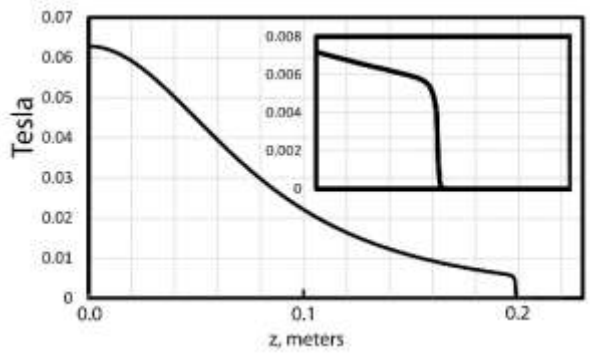

Figure 2 Axial magnetic field B_z of the model in Figure 1. Inset is a detail that shows the 'knee' of the magnetic field.

Starting at z=0, x=0, and y=10 microns the simulated electron trajectory moves smoothly along a field line with its distance from the axis in y given approximately by:

$$y = 10 * (0.06283/B_z)^{0.5} \text{ microns} \qquad (10)$$

With higher energy electrons there is a significant deviation from this relationship due to non-adiabatic behavior. This is seen in the additional deflection in the x direction.

Figure 3 shows the results of a simulation of a 2.0 eV electron leaving the central field parallel to the z axis with an initial y offset of 10 microns.

Figure 3 shows that the final angle of the trajectory in the y direction is largely determined by the curve in the trajectory following the field line. In contrast, the angle of the trajectory in the x direction is directly due to the force created by the termination of the field. The combination of the two deflection causes a rotation of the trajectory out of the y plane.

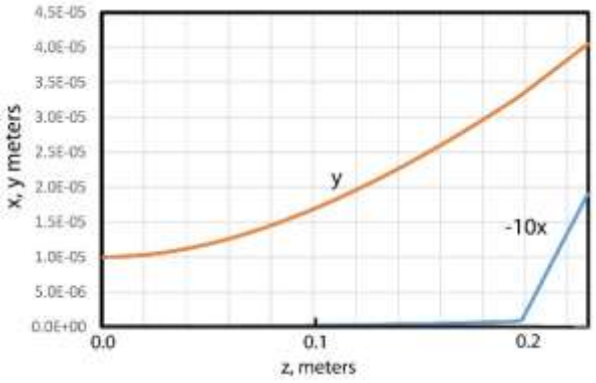

Figure 3 A simulated 2.0 eV electron trajectory resolved on the x and y axis for the model shown in Figure 1.

The angle of rotation is a constant of the model system, and does not depend on the starting position in x and y. The resultant angular images have two angular properties, the first in the direction of the magnetic vector potential (ϕ the transverse rotational direction, the x direction), and the second in the response to the magnetic field lines diverging from the axis at the field termination (θ the off-axis inclination, the y direction).

It can also be seen that the apparent position of the source of the angled trajectory is at a significantly different position along the z axis for the x and y directions. This shift in position makes a true focus of a bundle of trajectories around the axis impossible.

Figure 4 shows the forces in F_x and F_y in the area of the knee in the magnetic field. As the electron trajectory approaches the 'knee' in the magnetic field due to the opposing small loop field, it sees a rapid change in the magnetic field going to zero at the center of the second loop, and the trajectory is no longer adiabatic. The force due to the change in the vector potential in the x direction increases more than the force in the y direction, and the electron is deflected away from the axis.

The amount of the deflection depends on several factors: the initial magnetic field strength, the starting position in y at the first loop, the energy of the electron, and the position of the second loop which changes the value of Bz when the electron meets the 'knee' of the field. These are variables that can be manipulated when designing the instrument.

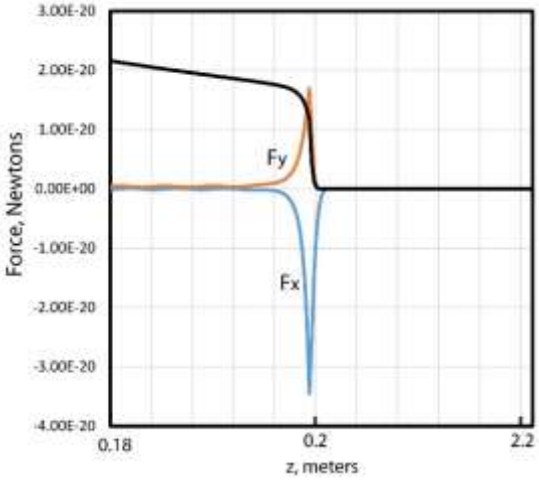

Figure 4 Resolved forces on an electron at the termination of the magnetic field: x (blue line), y (red line). The forces rapidly increase as the electron is driven away from the magnetic field line, and then decay as the electron leaves the field. The actual position of the magnetic field knee is shown superimposed as the black line.

We are looking for rules of thumb that can be used to simplify the design process. Currently we need to use a full calculation of the field and trajectories to estimate the microscope parameters such as angular magnification, and virtual image size. To extract the optical parameters from these calculations is very time consuming.

We want to create a metric that might be useful for designing the termination from just the shape of the magnetic field. We would like to predict the point of exit from the field, the angular magnification, the angle of rotation, and the trajectory bundle size. One possible approach is to use the equations 6 and 7. The off-axis forces at the termination are largely dependent on $\partial A_x/\partial z$, $\partial A_y/\partial z$, and the velocity in the z direction. We can recast this dependence as $\partial B_x/\partial z$, and the z velocity. Because the electrons follow a field line from the initial field, we expect that the forces will scale with the inverse of the root of the field strength at the termination and we can construct a metric related to the off-axis force:

$$\tilde{\mathcal{F}} = \frac{\partial B_Z}{\partial Z}\frac{\sqrt{E}}{\sqrt{B}} \qquad (11)$$

We might expect that the metric of equation 11 would give similar result at the exit field for different model parameters. Using a model system we can simulate a range of parameters. We choose a central solenoid of sufficient field strength to give a meaningful result, but not too strong that it would saturate a single layer ferromagnetic shield. There are many possible arrangements, and the model system used here is not intended to be an optimum design for an actual VPPEM. Two magnetic circuits are modelled to give different field strengths at the exit aperture.

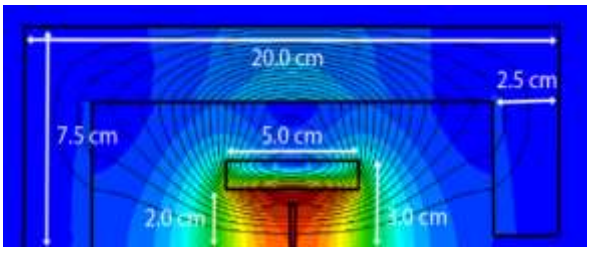

Figure 5 Model system of a solenoid in a ferromagnetic shield with an on-axis aperture. The ferromagnetic shield is 20.0 cm long, and 7.5 cm in radius, with a 2.5 cm thick 1018 steel shield. The solenoid is 5.0 cm long with a 2.0 cm inner radius and 3.0 cm outer radius.

The first magnetic circuit with dimensions are shown in Figure 5. The solenoid current produces an on-axis field maximum at the sample position of 0.5 Tesla. The field near the exit aperture at 7.5 cm is in the region of 0.02 Tesla.

The second magnetic circuit is the same as Figure 5 but with the shield length increased to 25 cm. The exit aperture is at 12.5 cm from the center, and the field at the aperture is an order of magnitude lower at 0.002 Tesla.

These two configurations give us a high, and low field termination for comparison. The other variables used in the calculations are aperture diameters 0.4 mm, 2.0 mm, and 2.0 cm, and electron energies 10.0 eV, and 100.0 eV.

The magnetic field and trajectories are modelled using Field Precision 2D TriComp suite of programs, and the colored plot of |B| shown in Figure 5 is imaged using 2D Infolytica MagNet software. We are interested in the angular magnification, and the relationship between θ and ϕ given these thee parameters of terminating field, aperture diameter, and electron energy.

Figure 6 shows the shape of the axial field, B_z, for the first magnetic field circuit, the high exit field configuration. Figure 6a shows a plot of B_z from the center of the solenoid at 0.0 cm to the end of the aperture at 10.0 cm. This plot is for the smallest aperture of 0.4 mm. The field decays smoothly from 0.5 Tesla until it reaches a 'knee' at approximately 0.25 Tesla near the aperture at 7.5 cm, and then decays rapidly to zero.

A comparison of the shape B_z for the three aperture sizes is shown in Figure 6b. Figure 6b shows that as the aperture becomes larger the 'knee' of the field in the region of the aperture at 7.5 cm becomes more rounded, and the field termination is less abrupt. For the 2.0 cm aperture, the field is somewhat lower at the aperture.

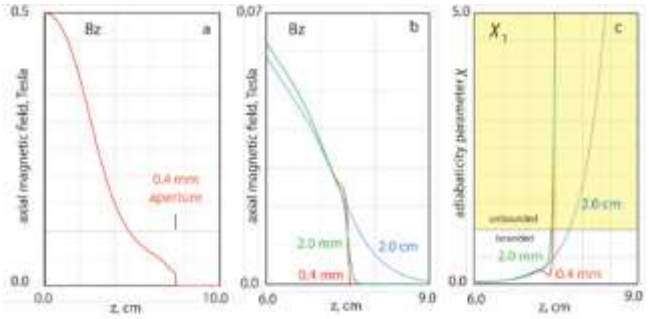

Figure 6 Comparison of the field shape for three different aperture sizes for the high field model of Figure 7, a) the axial field for a 0.4 mm aperture from the center of the solenoid at 0.0 cm to the end of the ferromagnetic shield at 10 cm, b) comparison of the axial field around the aperture position at 7.5 cm for three aperture sizes, c) comparison of the adiabaticity parameter for three aperture sizes.

Electrons can be accelerated in the strong magnet field without distorting the image. VPPEM normally images using very low energy electrons at the sample, typically around 1.0 eV. A sample bias is used to accelerate the electrons up to tens of electron volts at the aperture for insertion into the CHA input lens. This means that energy of the electrons at the exit aperture can be easily changed to manipulate the focal properties of the instrument. We have simulated electron trajectories over a range of electron energies, however, we only present the results for 10.0 eV and 100.0 eV. All results are for trajectories 1.0 micron off the axis at the center of the 0.5 Tesla field.

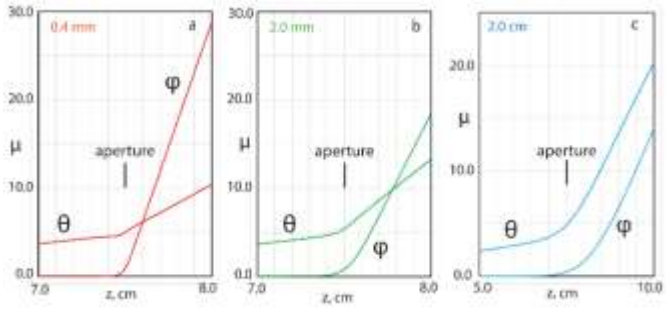

Figure 7 Trajectories for 10.0 eV electrons leaving the magnetic field of the high field model of Figure 5, a) aperture 0.4 mm ID, b) aperture 2.0 mm ID, c) aperture 2.0 cm ID. The in-plane deflection is ϕ, and the transverse out-of-plane deflection is θ. The position of the start of the aperture at 7.5 cm is indicated.

Figure 7 shows the trajectories for 10.0 eV electrons exiting from the three apertures for a 1 micron off-axis position at the sample, and the high field termination. The plots are for the in-plane θ deflection, and the out-of-plane ϕ deflection. There are some general trends as the aperture size increases, and the field termination becomes less abrupt. The radial deflection, Φ, decreases from 5.8×10^{-3} radians for the 0.4 mm aperture to 1.5×10^{-3} for the 2.0 cm aperture. At the same time, the relative sizes of the θ and ϕ deflection change. This leads to a change in the out-of-plane image rotation, Ψ, which changes from 76° for the 0.4 mm aperture to 42° for the 2.0 cm aperture. Table 1 summarizes the results for numerical simulations of the trajectories for the two field strengths, three aperture sizes, and two energies.

	High field			Low field		
	0.4 mm	2.0 mm	2.0 cm	0.4 mm	2.0 mm	2.0 cm
10.0 eV	$\Phi=5.8\times10^{-3}$ $\Psi=76^o$	$\Phi=4.2\times10^{-3}$ $\Psi=62^o$	$\Phi=1.5\times10^{-3}$ $\Psi=42^o$	$\Phi=1.8\times10^{-3}$ $\Psi=76^o$	$\Phi=1.8\times10^{3}$ $\Psi=73^o$	$\Phi=1.5\times10^{-3}$ $\Psi=53^o$
100.0 eV	$\Phi=1.9\times10^{-3}$ $\Psi=82^o$	$\Phi=1.5\times10^{-3}$ $\Psi=74^o$	$\Phi=9.0\times10^{-4}$ $\Psi=47^o$	$\Phi=6.6\times10^{-4}$ $\Psi=76^o$	$\Phi=6.5\times10^{-4}$ $\Psi=73^o$	$\Phi=5.9\times10^{-4}$ $\Psi=62^o$
Φ_{10}/Φ_{100}	3.05	2.73	1.64	2.73	2.71	2.56
Estimated Magnification at 10.0 eV	x4.45	x5.5	x10.7	x7.9	x8.1	x9.6
Estimated Exit field, T at 10.0 eV	2.52×10^{-2}	1.66×10^{-2}	4.40×10^{-3}	7.90×10^{-3}	7.60×10^{-3}	5.40×10^{-3}

Table 1 Results from electron trajectory calculations for two magnetic circuits based on Figure 3. The nominal high and low field values at the apertures are 0.02 and 0.002 Tesla respectively.

We can compare equation 11 with the results of table 1. Figure 8 is a plot of equation 11 for the three high field cases and 10 eV electrons.

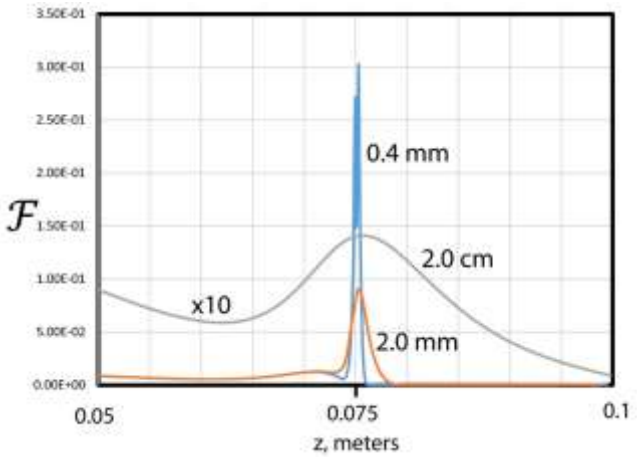

Figure 8 Plot of Equation 11 for three aperture sizes. High field termination with 10.0 eV electrons.

The general trends are clear, and this is very encouraging. However, we do not as yet understand how this metric could be useful for designing a microscope. This is work in progress and needs more investigation.

In conclusion, we have created a consistent mathematical description of the electron trajectories: within the field, on termination, and the final trajectory. This description makes it much clearer how the VPPEM image is created. This work might lead to a metric that could be used in microscope design.